



HAL
open science

Achieving superlubricity using selected tribo-pairs lubricated by castor oil and unsaturated fatty acids

Yun Long, Jules Galipaud, Volker Weihnacht, Stefan Makowski, Jean Michel Martin, Maria-Isabel De Barros Bouchet

► **To cite this version:**

Yun Long, Jules Galipaud, Volker Weihnacht, Stefan Makowski, Jean Michel Martin, et al.. Achieving superlubricity using selected tribo-pairs lubricated by castor oil and unsaturated fatty acids. *Tribology International*, 2022, 169, 10.1016/j.triboint.2022.107462 . hal-03956712

HAL Id: hal-03956712

<https://hal.science/hal-03956712>

Submitted on 22 Jul 2024

HAL is a multi-disciplinary open access archive for the deposit and dissemination of scientific research documents, whether they are published or not. The documents may come from teaching and research institutions in France or abroad, or from public or private research centers.

L'archive ouverte pluridisciplinaire **HAL**, est destinée au dépôt et à la diffusion de documents scientifiques de niveau recherche, publiés ou non, émanant des établissements d'enseignement et de recherche français ou étrangers, des laboratoires publics ou privés.



Distributed under a Creative Commons Attribution - NonCommercial 4.0 International License

Achieving superlubricity using selected tribo-pairs lubricated by castor oil and unsaturated fatty acids

Yun Long¹, Jules Galipaud^{1,2}, Volker Wehnacht³, Stefan Makowski³, Jean Michel Martin¹
and Maria-Isabel De Barros Bouchet^{1*}

¹ *University of Lyon, Ecole Centrale de Lyon, Laboratory of Tribology and System Dynamics,
CNRS UMR 5513, 36, Avenue Guy de Collongue 69134, Ecully Cedex, France*

² *University of Lyon, INSA de Lyon, Laboratoire MATEIS, CNRS UMR 5510, F-69621
Villeurbanne Cedex, France*

³ *Fraunhofer Institute for Material and Beam Technology IWS, Winterbergstraße 28, 01277
Dresden, Germany.*

*Corresponding author: maria-isabel.de-barros@ec-lyon.fr (Maria Isabel De Barros Bouchet),

Tel number: 00 33 472186280, Fax number: 0478433383)

Highlights

- The occurrence of superlubricity is governed by tribo-pair type in castor oil.
- Steel/a-C(30) pair is the best combination to minimize friction in castor oil.
- Fatty acid-based lubricants activate $-(\text{CH}_2-\text{CH}_2)_n-$ oligomers formation on a-C(30) surfaces except linoleic acid.
- Shearing a-C in fatty acid-based lubricants triggers a carbon re-hybridization from carbon sp^3 into sp^2 .

Abstract

Systematic friction tests have been performed to unveil the key factors for reaching superlubricity ($\text{CoF} < 0.01$) in the presence of unsaturated fatty acid-based lubricants under boundary lubrication regime. The impact of different tribo-pairs and lubricants has been investigated. When the counterpart is steel, results show that a hydrogen-free DLC coating is indispensable to achieve superlubricity in castor oil. Among pure unsaturated fatty acids as lubricants, oleic and ricinoleic acid gave superlow friction but linoleic acid is not recommended to lubricate steel/a-C contact due to the occurrence of high friction and wear. X-ray photoelectron spectroscopy (XPS) and X-Ray-Excited Auger Electron Spectroscopy (XAES) analyses reveal that hydrogen-free carbon can activate two pathways to passivate surface and to achieve superlubricity with fatty acid-based lubricants (i) carbon re-hybridization by forming a high-density sp^2 carbon network and (ii) $-(\text{CH}_2-\text{CH}_2)_n-$ oligomers formation on top surface. At the opposite, linoleic acid hinders the formation of $-(\text{CH}_2-\text{CH}_2)_n-$ oligomers and oxidizes carbon surfaces.

Keywords: Superlubricity, DLC, unsaturated fatty acid, $-(\text{CH}_2-\text{CH}_2)_n-$ oligomers, sp^2 carbon re-hybridization

1. Introduction

Current trend towards greater energy conservation and less environmental pollution encourages tribologists to discover eco-friendly substitutes for traditional toxic additives in lubricants such as zinc dialkyldithiophosphate [1], phosphate ester [2], sulphides [3], etc. This need has been met by replacing them with fatty acids, and fatty acid-based lubricant like glycerides. As natural components of animal fats and vegetable oils, they are non-toxic and well biodegradable. Moreover, friction improvement has been observed by adding them in mineral oil [4] and poly-alpha-olefin (PAO4) [5].

The excellent lubricity of fatty acids derives partially from its ability to form a self-assembled monolayer (SAM) on polar surfaces, such as steel [6] and glass [7]. Due to repulsion between SAMs, direct contact between two surfaces is avoided. It is noteworthy that SAM of fatty acid roots on steel surface by forming carboxylate groups [8], with both chain lengths [9] and function groups [10] governing the lubricity of fatty acids.

When fatty acids lubricate diamond like carbon (DLC), friction behavior is strongly associated with DLC type. For instance, self-mated hydrogenated DLC (a-C:H) lubricated by oleic acid shows a $CoF > 0.04$ while self-mated tetrahedral amorphous carbon (ta-C) reach superlubricity under the same conditions [11]. This phenomenon is accompanied by oleic acid molecules being detected on a:C-H but not on ta-C. It was later explained as high Young's modulus of ta-C causes an extreme local contact pressure, which drives fatty acids undergoing a cascade decomposition into small fragments [12]. This phenomenon is accompanied by graphitization of ta-C top surface [13] and surface passivation by fatty acid fragments.

Glycerides are esters composed of fatty acids and glycerol. It is the main component of vegetable oils like castor oil, sunflower oil, palm oil, etc. Unlike other vegetable oil, castor oil is composed of fatty acids with hydroxy group. It can maintain a CoF below 0.05 at high temperature (100°C) and load (0.92 GPa) while lubricating a steel/steel pair [14]. Zeng et al.

[15] reported superlubricity for a castor oil-lubricated Nitinol alloy/steel pair and attributed this to the formation of metal oxyhydroxides on both surfaces.

Another glyceride, Glycol monooleate (GMO), can significantly reduce friction when lubricating a ta-C surface. Adding 1% GMO in PAO4 then can reduce CoF from 0.09 to 0.02 for a steel/ta-C tribo-pair at boundary lubrication regime [16]. Kano M group shows that friction behavior of this tribo-pair at boundary lubrication regime is still governed by sliding speed. Superlubricity can be obtained when sliding speed is above 0.1 mm/s. And this superlubricity is explained by OH passivation of ta-C surface [17].

The previous studies of castor oil have focused on steel/steel tribo-pair. So, to verify its universality, we have compared its lubricity for seven different tribo-pairs: steel/a-C(30), steel/ta-C(55), steel/ta-C(62), steel/a-C:H, steel/SiC, steel/Si₃N₄, steel/steel. Afterwards, the best combination is selected to investigate the key factors of fatty acid lubrication mechanism. The purpose of this work is to unveil the correlation between tribo-pair type and fatty acid-based lubricant and then to provide guidance for industrial application.

2. Material and methods

2.1. Materials

As lubricants, castor oil, ricinoleic acid (purity $\geq 99\%$), linoleic acid (purity $\geq 99\%$) and oleic acid (purity $\geq 99\%$) abbreviated as CO, RA, LA, OA respectively, were obtained from Sigma-Aldrich (St. Louis, USA). Their molecular structures are shown in Fig.3c.

As for tribopairs, AISI 52100 steel pins with 100 mm radius spherical head are provided by Rocholl GmbH (Eschelbronn, Germany). They slide against 7 different counterparts. SiC, Si₃N₄ were produced by hot pressing and purchased from LianYunGang HighBorn Technology (LianYunGang, China). Steel discs are bought from PCS instruments (London, England). More details can be found in Table 1. SiC, Si₃N₄ and steel surfaces are used as received without further processing.

Hydrogen-free amorphous carbon coatings with three different contents of sp² and sp³ hybridized carbon atoms were deposited on steel flats surfaces by Fraunhofer IWS (Dresden, Germany) with plasma-filtered Laser-Arc™ technique [18] using a commercial PVD coating system. The variation of the sp² and sp³ contents was achieved by different deposition parameters. Starting from a standard ta-C coating, a harder variant was produced by using an additional bias voltage of -100 V and a softer variant was produced by additional heating at 145°C. The designations a-C(30), ta-C(55) and ta-C(62) were assigned from the measured indentation hardness values of the coatings 30 GPa, 55 GPa and 62 GPa, respectively. All three coatings were smoothed by lapping with diamond slurry to remove growth defects. Coating thicknesses of a-C(30), ta-C(55) and ta-C(62) are 3.2, 4.0, 3.5 μm, respectively. a-C(30) coating has been also prepared on steel pins. The roughness of a-C(30) coated pin is 8.5 nm. On the other hand, a-C:H samples with 20% hydrogen was manufactured by plasma enhanced CVD where acetylene gas is used as precursor [19]. And a-C:H coating thickness is 2 μm.

Table 1. Mechanical properties, and production information of flats in this study. H represents hardness, E is elastic modulus of coating, and ν is Poisson's ratio. To distinguish those three DLCs, they are named by DLC type followed by its hardness in parentheses.

| Flats type | Suppliers | Production method | H (GPa) | E (GPa) | ν |
|--------------------------------|----------------------|------------------------|---------|---------|-------|
| a-C(30) | Fraunhofer IWS | Filtered laser-arc PVD | 30 | 237 | - |
| ta-C(55) | | | 55 | 521 | - |
| ta-C(62) | | | 62 | 626 | - |
| a-C:H | | Plasma enhanced CVD | 29 | 260 | - |
| steel | PCS instruments | - | 8 | 210 | 0.3 |
| Si ₃ N ₄ | LianYunGang HighBorn | Hot pressing | 16 | 310 | 0.27 |
| SiC | Technology | | 25 | 410 | 0.18 |

2.2. Friction and wear experiments

Tribological tests are performed on a linear reciprocating tribometer [20] with pin-on-flat configuration. The flat is fixed and sliding speed of pin follows a sine function. When the speed of pin reaches its maximum at the midst of a stroke, we record this speed as maximum sliding speed. In this work, maximum speed is adjusted to 3 mm/s, insuring that tribo-tests are conducted under boundary lubrication regime. The tangential force is monitored by a piezoelectric sensor and recorded at 3 mm/s to calculate friction coefficient (CoF) with an accuracy of ± 0.001 . All experiments are conducted 3 times.

Before friction tests, all samples are sonicated in n-heptane bath for 30 minutes, then in acetone for 5 minutes. After cleaning and installation of samples in the tribometer, the contact between pin and flat is fed with 50 μ L of lubricants. As for experimental conditions, temperature is fixed at 100°C for tests located before Fig. 6 and initial maximum Hertzian contact pressure (Pmax) is about 295 MPa. Besides 100°C, other temperatures like 50°C and 60°C are used for tests in Fig.6. Since elastic modulus and Poisson's ratio varies with tribo-pairs, the applied normal force was adjusted to reach the same Pmax (detailed in Table 2). Additionally, the stroke length of tests is adjusted at 3 mm.

2.3. Surface analyses

After tribo-tests, samples are rinsed with n-heptane to remove lubricant residuals and they are optically imaged by digital microscopy (VHX-6000, Keyence, Osaka, Japan).

Their 3D topographical information is captured by interferometer (ContourGT-K1, Bruker, Billerica, USA) using VXI mode. For 3D topographical profile, an area of 126 x 95 μm^2 is recorded with 50x objective magnification and a x/y resolution of 0.2 μm and z resolution of <0.1 nm. Roughness Sa is calculated by Vision64 software. A larger area of 2334 x 1749 μm^2 is recorded with x 2.75 objective magnification to acquire radius of curvature inside the wear scar, where outside wear scar is masked.

XAES/XPS is used to record the change of surface chemistry by comparing outside and inside wear scar. This XAES/XPS apparatus is equipped with a ULVAC-PHI Versa Probe II spectrometer using an Al K α X-ray source (1486.6 eV). Quantification was carried out using the transmission function of this apparatus and an angular distribution correction for 45° angle. Sensitivity factors were extracted from [21], where cross section and escape depth correction were integrated. Hence, surface analysis is performed at take-off angle of 45 ° and with a probed area of 200 x 200 μm^2 . To minimize noise, spectra of C1s, O1s, CKLL are accumulated under pass energy of 23.5 eV. Afterward, Shirley background are adopted to remove background from peaks by Multipack software. For steel surfaces, iron oxide peak from O1s is used to calibrate spectrum by indexing it at 530.0 eV [22], while XAES/XPS spectra of DLC samples are calibrated by fixing C-C/C=C contribution of C1s at 284.8 eV. In this study, the first derivation of CKLL spectra has been smoothed by Savitzky-Golay filter.

Invia™ Raman spectroscopy purchased from Renishaw (UK) is also used in this study. Spectra are acquired on three spots, each randomly selected inside and outside of the wear scar by adopting 633 nm laser. Laser power was kept below 10 mW at the sample surface to ensure that excitation energy was below damage threshold.

3. Experimental Results

3.1. Influence of tribo-pair materials under castor oil lubrication

Seven different tribo-pairs: steel/a-C(30), steel/ta-C(55), steel/ta-C(62), steel/a-C:H,

steel/SiC, steel/Si₃N₄, steel/steel have been investigated lubricated by castor oil. For steel sliding against steel, Si₃N₄, and SiC, friction curves follow the same trend i.e., a friction coefficient (CoF) increasing with sliding time (Fig. 1a). After 1.1h sliding, CoF reaches 0.055, 0.031 and 0.085, respectively. Such a friction increase is accompanied by the generation of black scratches (Fig. 1c) on steel wear scars. As a result, final roughness Sa of steel wear scars significantly increases (Table 2). For instance, when steel slides against steel, roughness of steel pin increases from 6.6 nm to 92 nm when comparing steel surface before and after friction. However, depending on the type of tribo-pairs, the nature of those black substances in the wear scar are different.

From Raman analysis (Fig. 2), the characteristic peak of Fe₃O₄ [23] is observed at 672 cm⁻¹ for steel pin rubbed against steel. Fe₃O₄ is also present at steel surface rubbed against Si₃N₄. But other peaks located at 222, 289, 408, 1315 cm⁻¹ indicate that α-Fe₂O₃ [24] is also present in steel wear. An additional peak at 1585 cm⁻¹ corresponds to carbon G-band, which is commonly detected in the composite of α-Fe₂O₃ and carbon [25].

Concerning steel/SiC pair, only carbon D and G peaks are detected in steel wear scar, suggesting a carbonaceous transfer layer, with SiC and the lubricant being possible carbon sources.

In brief, when steel slides against steel, SiC or Si₃N₄, iron oxide or/and carbonaceous substance accumulate on steel surface and form a rough topography. This leads to more severe conditions because the lambda parameter, describing the ratio of lubricant film thickness over surface roughness, decreases.

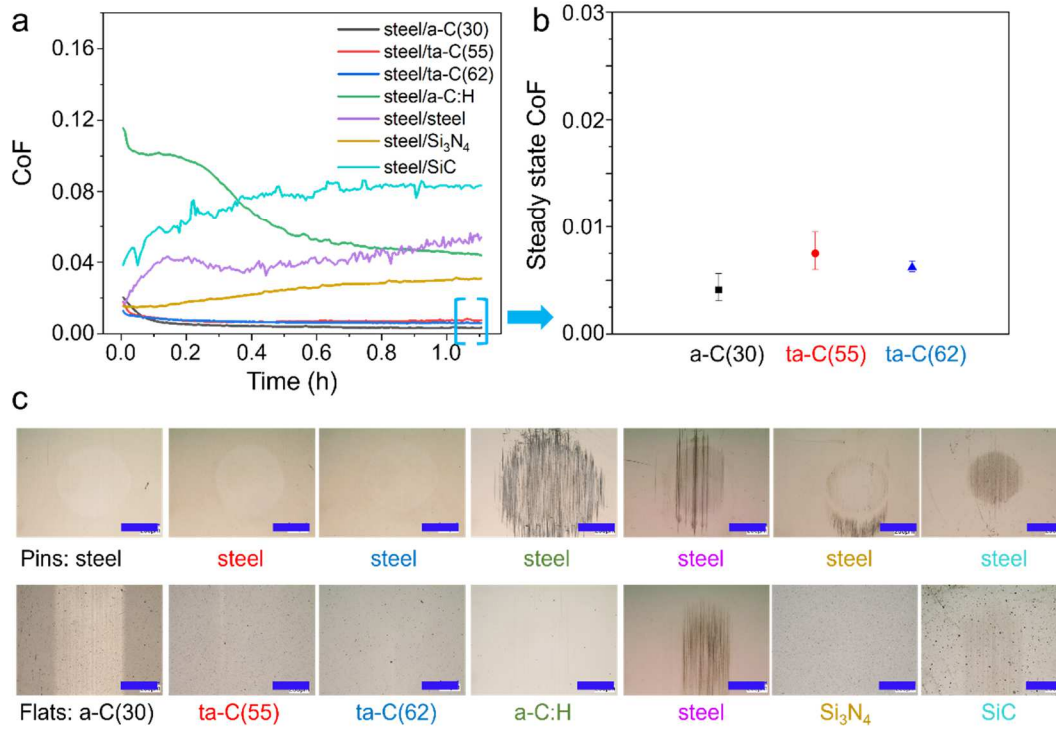


Figure 1. **a** Friction tests of different tribo-pairs lubricated by castor oil at 100°C. **b** a comparison of steady state CoF of three different superlubricity experiments. Error bar refers to the largest and lowest CoF obtained in 3 repeating tests. **c** optical images of tribo-pairs' wear scars. The scale bar corresponds to 400 μm .

Contrary to the previous trend, when steel slides against DLC coatings (Fig. 1a), CoF decreases with sliding time and after running-in period, CoF reaches a steady state and becomes independent of time. Among them, the case of a-C:H shows the highest CoF (0.044) and wear scar on steel is covered by black scratches (Fig. 1c). The wear scar diameter at the end of the test is 1.58 times larger than the Hertzian one at the beginning of the test, indicating substantial wear. Like the case of steel/SiC, black substances are composed of amorphous carbon (Fig. 2) and this causes a rise of steel surface roughness.

Table 2. Detailed information of different tribo-pairs lubricated by castor oil that concerns normal force (F_n), friction (CoF), wear, roughness change (S_a), liquid film thickness (h_c). Diameter of wear and Hertzian contact have been abbreviated as D_w and D_H . When D_H of steel/DLCs is calculated, E and ν of steel are used to represent those parameters of DLC discs as DLC coatings are deposited on steel with a thickness $\leq 4 \mu\text{m}$ (more details are illustrated in SI. Table 4). R_w is the radius of curvature inside the wear scar. The calculation of h_c and lambda ratio are calculated with the parameters recorded after friction test and are detailed in

supplementary information (SI). Information listed in this table refers to one test of repeated experiments series.

| | Steel/ a-C(30) | | Steel/ ta-C(55) | | Steel/ ta-C(62) | | Steel/ a-C:H | | Steel/ Steel | | Steel/ Si ₃ N ₄ | | Steel/ SiC | |
|------------------------------------|-------------------|------|--------------------|------|--------------------|------|-----------------|------|-----------------|------|--|------|---------------|------|
| F_n (N) | 100 | | 100 | | 100 | | 100 | | 100 | | 71 | | 60 | |
| CoF at 1.1h | 0.004 | | 0.007 | | 0.006 | | 0.044 | | 0.055 | | 0.031 | | 0.085 | |
| | Pin | Flat | Pin | Flat | Pin | Flat | Pin | Flat | Pin | Flat | Pin | Flat | Pin | Flat |
| D_w (μm) | 843 | 807 | 828 | - | 841 | - | 1269 | 778 | 812 | 785 | 701 | - | 634 | 660 |
| D_H (μm) | 804 | | 804 | | 804 | | 804 | | 804 | | 678 | | 622 | |
| D_w/D_H | 1.05 | 1.00 | 1.03 | - | 1.05 | - | 1.58 | 0.97 | 1.01 | 0.98 | 1.03 | - | 1.02 | 1.06 |
| R_w (μm) | 105 | - | 110 | - | 112 | - | 118 | - | 136 | - | 112 | - | 107 | - |
| Sa before (nm) | 6.6 | 11.2 | 6.6 | 8.0 | 6.6 | 8.2 | 6.6 | 5.0 | 6.6 | 4.4 | 6.6 | 12.4 | 6.6 | 9.6 |
| Sa after (nm) | 5.2 | 9.0 | 4.9 | 9.2 | 5.1 | 10.2 | 125 | 23 | 92 | 14 | 13.2 | 12 | 20 | 20 |
| h_c (nm) | 4.9 | | 5.0 | | 5.1 | | 5.2 | | 5.6 | | 5.2 | | 5.2 | |
| Lambda | 0.47 | | 0.48 | | 0.45 | | 0.04 | | 0.06 | | 0.29 | | 0.18 | |

Interestingly, once a-C:H is replaced by hydrogen-free carbon, superlubricity is achieved. The lowest CoF as 0.004 is obtained by sliding steel/a-C(30) friction pair, which is also significantly smaller than CoF of a-C(30)/a-C(30) friction tests (SI, Fig 2). When steel slides against a-C(30), steel pin is polished from 6.6 to 5.2 nm (Table 2). However, when a-C(30) slides against a-C(30), a-C(30) pin becomes rougher after friction and owns a roughness of 9.8 nm. Such difference in roughness triggers more asperities coming into contact, hence, resulting in a higher CoF. Both steel and a-C(30) wear scars are homogeneously colored (Fig. 1c) and polished (Table 2). The final roughness of steel and a-C(30) are inferior to 10 nm, and lambda ratio stays below unity indicating that steel/a-C(30) pair is lubricated under boundary lubrication regime. Regarding other two hard ta-Cs, only slight scratches have been remarked

on the surface after friction and their surface roughness slightly increases after friction. The difference in optical images between a-C(30) and ta-Cs is likely to originate from their hardness difference. On the steel side, no matter sliding against a-C(30) or ta-Cs, Raman spectra performed in steel wear scar are identical as the one outside of wear scar, indicating that no carbonaceous transfer layer has formed (Fig. 2). As Raman has limited surface sensitivity, XPS/XAES will be used in the following. Results are shown in the following section.

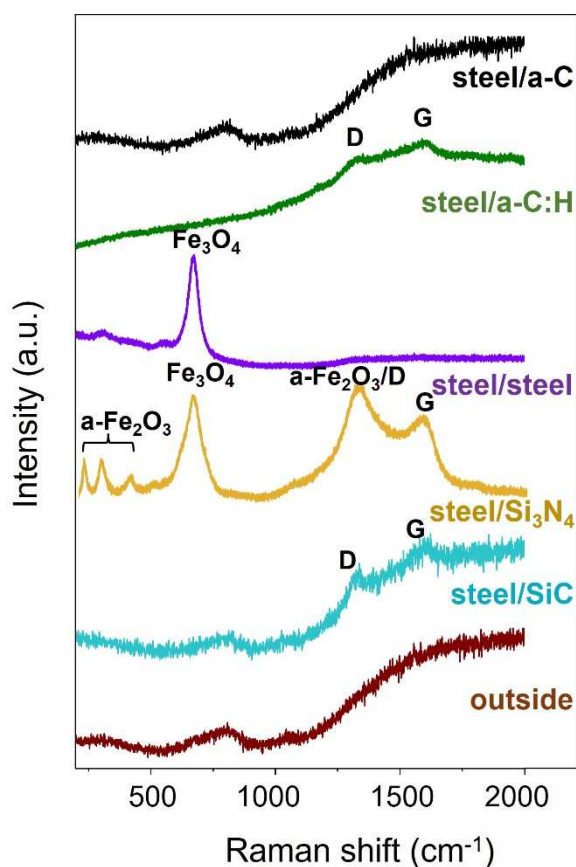


Figure 2. Raman spectra of black substances in steel wear scar on pin for different tribo-pairs. As for steel's counterparts being hydrogen-free amorphous carbon, analysis spots are randomly taken inside steel wear scars due to lack of black substances. Steel/a-C pair shares the similar Raman spectra as steel/ta-Cs in steel wear scar.

3.2. Impact of lubricants on steel/a-C(30) tribopair

Due to the lowest friction measured of all pairs with castor oil, steel/a-C(30) pair is chosen to investigate how function groups present in different fatty acids influence its tribological performance. In castor oil (CO), oleic acid (OA) and ricinoleic acid (RA), CoF decreases

drastically and stabilizes after a short running-in period (Fig. 3a). On the contrary, linoleic acid (LA) induces a rise of CoF after 0.2h sliding and CoF stabilizes at around 0.055. Briefly, regarding steel/a-C(30) pair, the lowest friction of the four lubricants follows this sequence: CO<RA<OA<<LA. Better performance of CO may partially originate from its greater viscosity and capacity to provide a thicker liquid film (about 5nm in Table 3). The same order is also found for wear, with CO showing no wear and LA the highest wear. Comparing four lubricants, only the steel pin lubricated by CO shows a wear beyond detection limit by interferometry (Fig.3b). Steel pins lubricated by the other three lubricants show average wear depths from 100 nm to 190 nm, corresponding to a color change from light blue to dark blue. Their optical images are shown in SI. Fig. 1. Friction tests trigger a change of surface roughness and radii of wear scar curvature, however, lambda ratio of the four tests stay always far below unity meaning that their lubrication regime is under boundary lubrication.

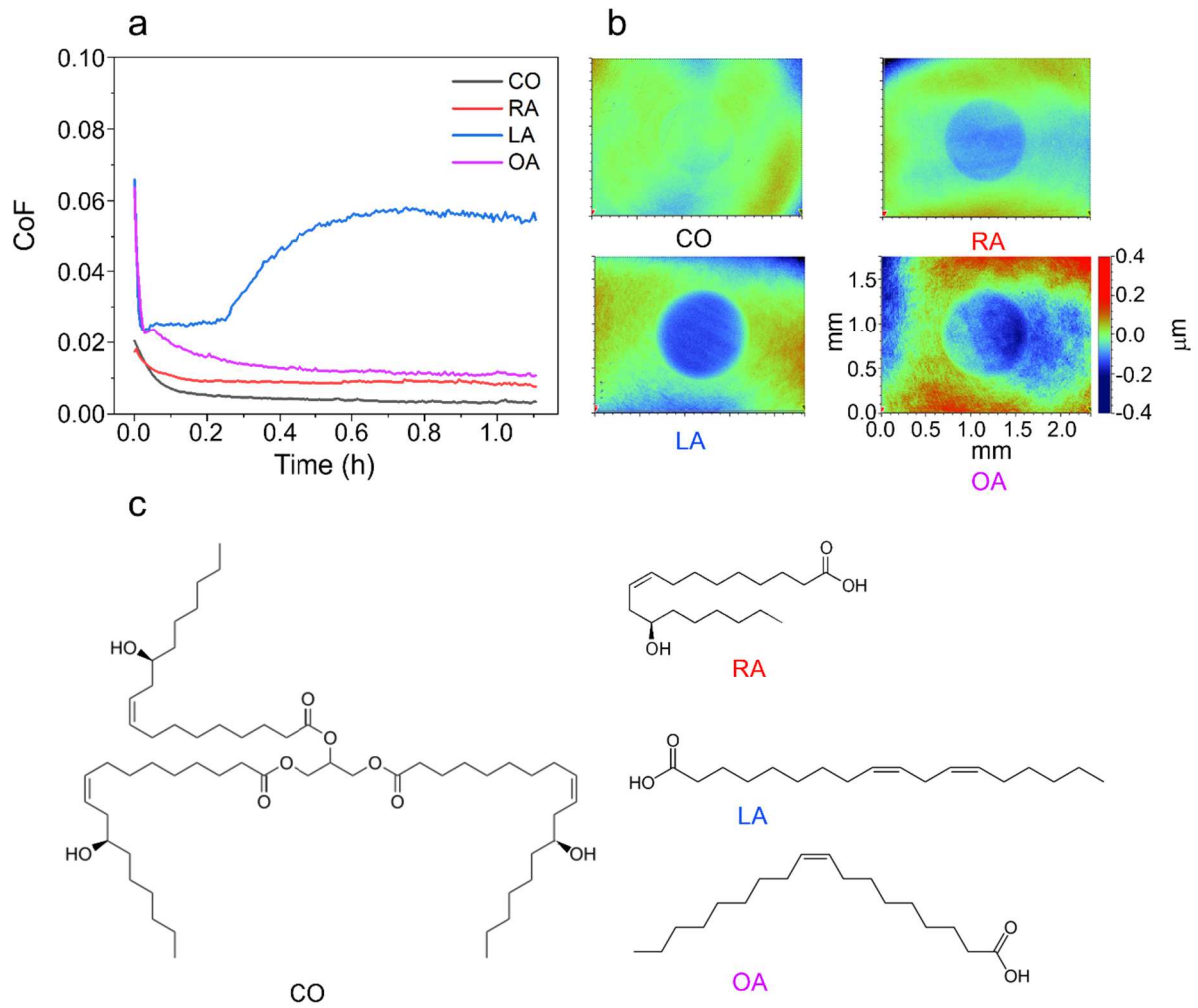


Figure 3. **a** friction curves of steel/a-C(30) lubricated by CO, RA, LA and OA at 100°C **b** 3D profile images after fitting with a spherical curve of steel wear surfaces. Negative value colored in blue means material missing from steel surface. **c** molecular structures of 4 lubricants. Here, triester of glycerol and ricinoleic acid is used to represent CO molecular structure since its content is superior to 85% in CO.

Table 3. friction and wear information of steel/a-C(30) lubricated by castor oil at 100°C.

Their viscosities at 100°C are obtained from [26,27,28].

| | CO | | RA | | LA | | OA | |
|----------------------------|--------------|------|--------------|------|--------------|------|--------------|------|
| Viscosity@100°C (mPa·s) | 18.0 | | 11.1 | | 3.3 | | 5.0 | |
| CoF @ 1.1h | 0.004 | | 0.008 | | 0.055 | | 0.011 | |
| | Pin | flat | Pin | flat | Pin | flat | Pin | flat |
| D _w (μm) | 843 | 807 | 900 | 876 | 1056 | 987 | 892 | 830 |

| | | | | | | | | |
|-------------------------|-------------|------|-------------|------|-------------|------|-------------|------|
| D_H (μm) | 804 | | 804 | | 804 | | 804 | |
| D_w/D_H | 1.05 | 1.00 | 1.12 | 1.09 | 1.31 | 1.23 | 1.1 | 1.0 |
| R_w (μm) | 105 | | 117 | | 151 | | 106 | |
| Sa before (nm) | 6.6 | 11.2 | 6.6 | 11.2 | 6.6 | 11.2 | 6.6 | 11.2 |
| Sa after (nm) | 5.2 | 9.0 | 10.8 | 10.5 | 10.4 | 11.3 | 6.8 | 7.6 |
| h_c (nm) | 4.9 | | 3.3 | | 1.8 | | 1.9 | |
| Lambda | 0.47 | | 0.22 | | 0.12 | | 0.19 | |

XPS is used to unveil how lubricants control tribochemical reactions of steel/a-C(30). On the steel pin, only carbon (C), oxygen (O), and iron (Fe) are detected regardless of analysis location. With all lubricants, iron content is greater inside the pin wear scar than outside wear (SI Table 1). This increase is partially compensated by oxygen content decrease, except the case of LA, where oxygen content remains as high as 43% after friction.

Concerning steel pin lubricated by LA, O1s peak displays iron oxide (FeO_x) at 530.0 eV and iron hydroxide at 531.3 eV. However, their contents decrease after friction. It is the rise of C=O, C-O bonds at 532.2, 533.2 eV that maintains oxygen content unchanged (Fig. 4). Correspondingly, C-O, C=O bonds peaking at 286.3, 287.4 eV from C1s peak become more pronounced after friction. Steel pin also has a strong O-C=O bond contribution at 288.7 eV, whose content is 1.5 times greater than C-O bond. Regarding steel pins lubricated by CO, RA, OA, their ratio between O-C=O/C-O is less than 1.2. And only for steel lubricated by CO, C-O content is higher than O-C=O. Furthermore, FeOH peak is the strongest peak over other contributions from O1s. These results suggest that castor oil can facilitate formation of OH termination on steel surface.

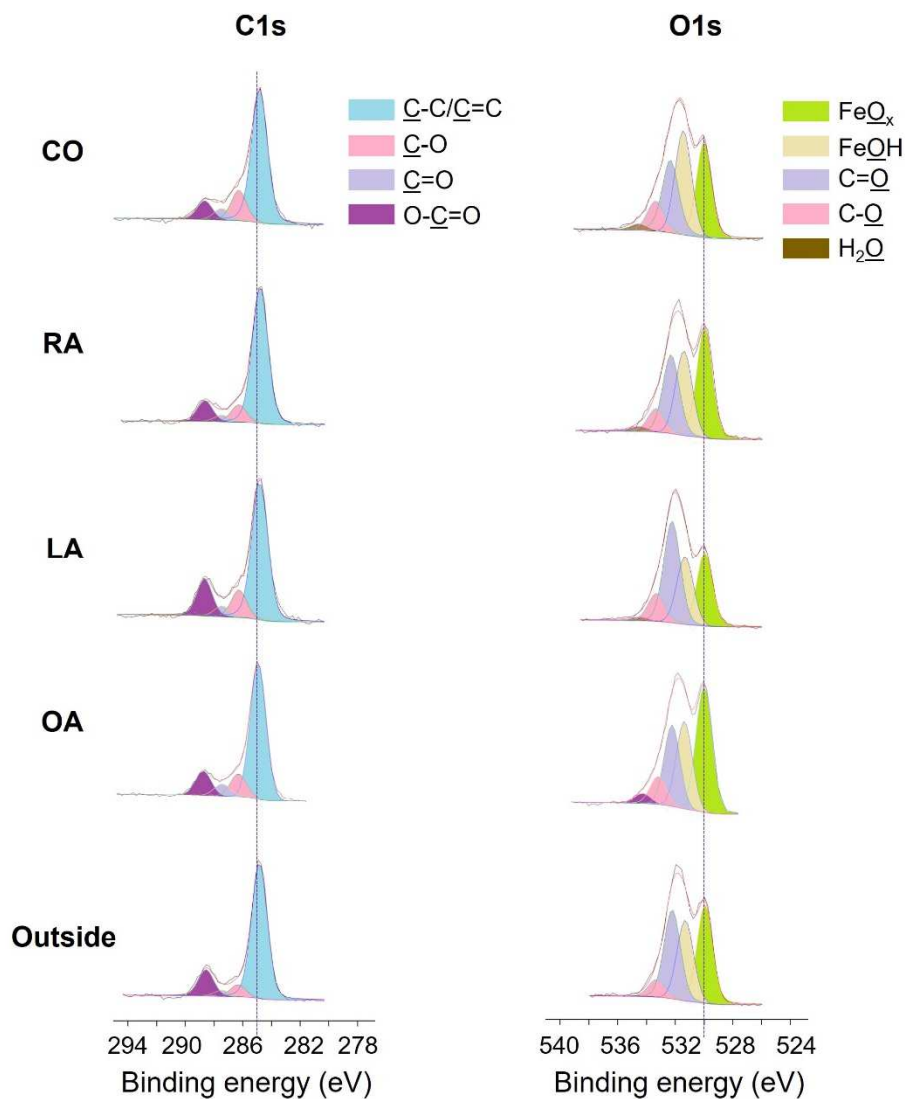


Figure 4. C1s and O1s XPS spectra of steel wear scars after friction tests of a-C(30)/steel pair in different lubricants: castor oil (CO), oleic acid (OA), ricinoleic acid (RA) and linoleic acid (LA), XPS spectra of outside wear scar is also shown.

On the a-C(30) flat, only carbon and oxygen are detected by XPS (Figure 5). Lower oxygen content has been recorded inside the wear track compared to outside, except for a-C(30) lubricated by LA (SI Table 2) in which oxygen content increases after friction. C1s peak also shows that peaks of C-O, C=O, and O-C=O at 286.3, 287.4, 288.6 eV are more pronounced inside the wear track (LA) compared to outside (Fig.5). And C-C/C=C peak at 284.8 eV is weaker. It is worthy to mention that the peak at 284.8 eV contains also signal from C-H. On the contrary, C-C/C=C peak for a-C(30) lubricated by CO, RA and OA is more intense than its content outside wear. In brief, sliding with CO, RA and OA triggers an

increase of carbon-carbon or carbon-hydrogen bonds for a-C(30) while sliding in LA provokes an increase of carbon-oxygen bonds.

However, regardless of lubricants, full width at half maximum (FWHM) of C-C/C=C peak in the wear track increased by 0.2 eV (SI Table 2) compared to outside. The change of FWHM correlates to the change of ratio between C-C and C=C. This ratio can be quantitatively evaluated by D parameter from the first derivation of CKLL Auger peak by a linear function [29]. Here, D parameter refers to the kinetic energy difference between the highest and lowest point in first derivation of CKLL [30]. D parameter of outside wear track is 16.0 eV (Fig.5). a-C(30) shearing in those four lubricants enlarges its D parameter. The highest D parameter is 18.6 eV obtained by a-C(30) lubricated by CO. Based on the fact that the D values of graphite and diamond are 20.0 [18] and 14.2 eV [31], 2.6 eV difference between inside and outside the wear track corresponds to a 31% difference in sp^2 content.

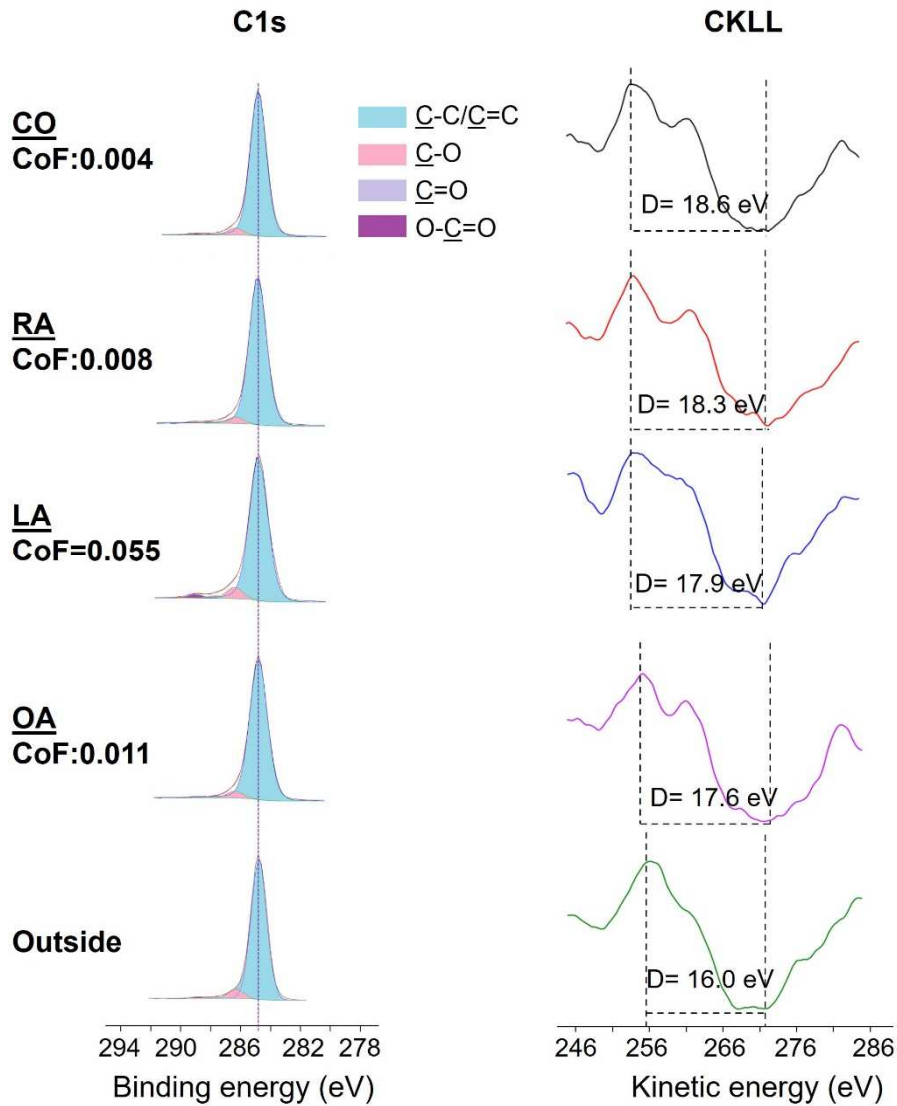


Figure 5. C1s XPS spectra of a-C(30) wear scars after friction tests in different lubricants.: castor oil (CO), oleic acid (OA), ricinoleic acid (RA) and linoleic acid (LA), The first derivation of XAES CKLL spectra is shown on the right side. Spectra of outside wear scar is also displayed for comparison.

Interestingly, a significant shoulder peak at 261 eV in the first derivation of CKLL spectra has been detected for a-C(30) surface lubricated by CO, RA and OA. From literature, polyethylene (PE) and PE-polyacetylene (PA) mixture also shares this peak but not PA alone [32]. For DLC, this peak has been reported to exist in DLC fabricated by ethylene [33] and it has been recently interpreted as being a characteristic peak of $-(\text{CH}_2-\text{CH}_2)_n-$ oligomer [18]. It is important to highlight that this peak is negligible in both outside wear and a-C(30) lubricated by LA (showing no superlow friction). This $-(\text{CH}_2-\text{CH}_2)_n-$ oligomer likely

originates from the defragmentation of fatty-acid based lubricants, since a full chain absorption of fatty acid will cause a rise of C=O and O-C=O bonds, but at C1s peak, those two bonds are negligible when a-C(30) surface lubricated by CO, RA and OA. The information depth of XAES CKLL is only 1.5 nm in our working conditions (SI. XPS information depth calculations).

4. Discussions

Lowest friction with castor oil lubrication out of all seven tribo-pairs studied can be obtained by mating steel with hydrogen-free DLC film (Fig. 1a), Friction reduction is attributed to steel surface polishing and prevention of material transfer. Indeed, neither local formation of iron oxide nor carbon film transfer will increase local roughness and deteriorate lubrication condition. This result agrees with the work of Quinchia [13], where they report $CoF > 0.05$ for steel/steel pair lubricated by castor oil in boundary lubrication regime. It also matches with the fact that the presence of iron oxide wear debris on steel surface will cause a rise of CoF [34].

In the case of steel /a-C:H pair, a carbonaceous transfer film will form on the steel surface, effectively changing the material pairing. This latter contact type has been proved to give higher CoF than self-mated ta-C contact in fatty acid-based lubricant [11]. Therefore, hydrogen-free carbon film is recommended to be applied with castor oil.

Besides the tribo-pair, the choice of lubricant is also important as it determines the chemistry of top surface. Among steel/a-C(30) pair lubricated with CO, RA, LA and OA, LA gives the highest CoF and the largest wear at 100 °C (Fig. 3). To ensure that their tribological difference does not derive from viscosity difference at the fixed temperature, experiments were conducted at a similar viscosity of 10.7 ± 0.4 mPa·s [27][28] by adapting testing temperature for each lubricant. After a short running-in, steel/a-C(30) lubricated by RA and OA, CoF stabilizes at 0.005 and 0.006, respectively (Fig. 6). However, steel/a-C(30)

lubricated by LA shows a CoF of 0.011 which is low, but nearly 2 times more than the case of RA and OA. Therefore, low viscosity is not the essential cause of LA's reduced lubrication ability and suggests a chemical interaction with the surface that is different from RA and OA. In fact, when steel/a-C(30) is lubricated by LA, it is associated with an oxidization of both steel and a-C(30) surfaces (Fig. 4, 5) and an absence of $-(\text{CH}_2-\text{CH}_2)_n-$ oligomer signal on a-C(30) surface. Oxidization of these surfaces is mainly from surface coverage by carbon-oxygen bonds. Opposite to the other 3 lubricants, LA is less stable towards oxidization. Driven by oxidation, LA can form chains with two COOH functions [35]. This explains the remarkable contribution of O-C=O bond in a-C and steel wear scar (Fig. 4, 5).

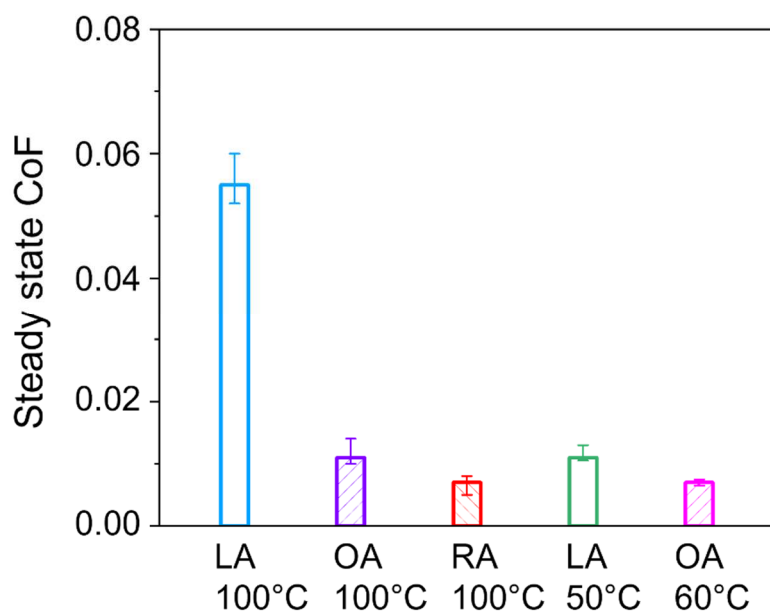


Figure 6. Correlation between steady state CoF and lubricants under different temperatures for steel/a-C(30) pair. Regarding RA at 100°C, LA at 50°C, and OA at 60°C, their viscosities are similar. It ensures that liquid film thickness of them is around 3 nm.

In this study, at 100°C, when CoF is less than or equal to 0.011, $-(\text{CH}_2-\text{CH}_2)_n-$ oligomer signal is detected on a-C(30). Once this signal becomes negligible, CoF is far beyond superlubricity regime (Fig. 3, 5). Such a good correlation between CoF and $-(\text{CH}_2-\text{CH}_2)_n-$ oligomer indicate CH_x oligomers to be a crucial factor to determine friction in fatty acid-

based lubricants. Previous study has demonstrated that superlubricity of self-mated a-C:H in vacuum is also accompanied by the detection of $-(\text{CH}_2\text{-CH}_2)_n-$ oligomer in a-C:H wear scar [18]. Concerning how $-(\text{CH}_2\text{-CH}_2)_n-$ oligomer lubricates the contact, further study will be conducted in the future.

It is important to highlight that an increase of sp^2 content has been recorded on a-C(30) top surface after shearing in CO, RA, LA and OA. This could correspond to a partial aromatization of a-C(30) [12] and it partially realizes surface passivation and avoids direct contact between surfaces [11]. However, the reduced lubrication properties of LA reveal that forming a top surface rich of sp^2 carbon are not the only factor to determine friction in fatty acid-based lubricants, as termination of carbon is also important.

5. Conclusion

This work highlights three key factors for achieving superlubricity in fatty acid-based lubricants: (i) maintaining low roughness of tribo-pair by avoiding oxidation or tribofilm formation, (ii) enriching top surface by sp^2 carbon, and (iii) passivating upmost carbon surfaces by $-(\text{CH}_2\text{-CH}_2)_n-$ oligomers. Such beneficial conditions can be achieved by using material tribopairs combining steel and non-hydrogenated DLC. The steel/a-C(30) pair lubricated with CO, OA or RA appears to be the most effective in terms of the superlubricity level, as a very effective polishing of the both antagonists is observed in these cases. In addition, interfacial shearing of the a-C(30) leads to a re-hybridization of the sp^3 carbon atoms to sp^2 and activates the decomposition of the lubricants triggering the formation of $-(\text{CH}_2\text{-CH}_2)_n-$ oligomers on the a-C(30).

Acknowledgements

This research was supported by TOTAL, Solaize Research Center and Federal Ministry of Economic Affairs and Energy Germany (BMWi) within project CHEOPS3 (Funding number 03ET1286B).

List of references

- [1] Henry JA. Composition and toxicity of petroleum products and their additives. *Hum Exp Toxicol* 1998; 17(2): 111-123. <https://doi.org/10.1177/096032719801700206>.
- [2] Cleveland L, Mayer FL, Buckler DR, Palawski DU. Toxicity of five alkyl-aryl phosphate ester chemicals to four species of freshwater fish. *Environ Toxicol Chem Int J* 1986; 5(3): 273-282. <https://doi.org/10.1002/etc.5620050306>.
- [3] Dooley AE. Toxicity of petroleum product additives. *Arch Environ Health Int J* 1963; 6(3): 324-328. <https://doi.org/10.1080/00039896.1963.10663402>.
- [4] Wells HM, Southcombe JE. *The theory and practice of lubrication: the " Germ" process*. Central House; 1920.
- [5] Loehle S, Matta C, Minfray C, Le Mogne T, Martin JM, Iovine R, Obara Y, Miura R, Miyamoto A. Mixed lubrication with C18 fatty acids: effect of unsaturation. *Tribol Lett* 2014; 53(1): 319-328. <https://doi.org/10.1007/s11249-013-0270-3>.
- [6] Simič R, Kalin M. Adsorption mechanisms for fatty acids on DLC and steel studied by AFM and tribological experiments. *Appl Surf Sci* 2013; 283: 460-470. <https://doi.org/10.1016/j.apsusc.2013.06.131>.
- [7] Minami I, Furesawa T, Kubo T, Nanao H, Mori S. Investigation of tribo-chemistry by means of stable isotopic tracers: Mechanism for durability of monomolecular boundary film. *Tribol Int* 2008; 41(11): 1056-1062. <https://doi.org/10.1016/j.triboint.2008.01.011>.
- [8] Loehlé S, Matta C, Minfray C, Le Mogne T, Iovine R, Obara Y, Miyamoto A, Martin JM. Mixed lubrication of steel by C18 fatty acids revisited. Part I: Toward the formation of carboxylate. *Tribol Int* 2015; 82: 218-227. <https://doi.org/10.1016/j.triboint.2014.10.020>.
- [9] Jahanmir S. Chain length effects in boundary lubrication. *Wear*, (1985). 102(4), 331-349. [https://doi.org/10.1016/0043-1648\(85\)90176-0](https://doi.org/10.1016/0043-1648(85)90176-0).
- [10] Loehlé S, Matta C, Minfray C, Le Mogne T, Iovine R, Obara Y, Miyamoto A, Martin JM. Mixed lubrication of steel by C18 fatty acids revisited. Part II: Influence of some key parameters. *Tribol Int* 2016; 94: 207-216. <https://doi.org/10.1016/j.triboint.2015.08.036>.
- [11] Kano M, Martin JM, Yoshida K, De Barros Bouchet MI. Super-low friction of ta-C coating in presence of oleic acid. *Friction* 2014; 2(2): 156-163. <https://doi.org/10.1007/s40544-014-0047-1>.
- [12] Kuwahara T, Romero PA, Makowski S, Wehnacht V, Moras G, Moseler M. Mechano-chemical decomposition of organic friction modifiers with multiple reactive centres induces superlubricity of ta-C. *Nat Commun* 2019; 10(1): 1-11. <https://doi.org/10.1038/s41467-018-08042-8>.
- [13] De Barros Bouchet MI, Martin JM, Avila J, Kano M, Yoshida K, Tsuruda T, Bai S, Higuchi Y, Ozawa N, Kubo M, Asensio MC. Diamond-like carbon coating under oleic acid lubrication: Evidence for graphene oxide formation in superlow friction. *Sci Rep* 2017; 7(1): 1-13. <https://doi.org/10.1038/srep46394>.

- [14] Quinchia LA, Delgado MA, Reddyhoff T, Gallegos C, Spikes HA. Tribological studies of potential vegetable oil-based lubricants containing environmentally friendly viscosity modifiers. *Tribol Int* 2014; 69: 110-117. <https://doi.org/10.1016/j.triboint.2013.08.016>.
- [15] Zeng Q, Dong G, Martin JM. Green superlubricity of Nitinol 60 alloy against steel in presence of castor oil. *Sci Rep* 2016; 6(1): 1-9. <https://doi.org/10.1038/srep29992>.
- [16] Tasdemir HA, Wakayama M, Tokoroyama T, Kousaka H, Umehara N, Mabuchi Y, Higuchi T. Ultra-low friction of tetrahedral amorphous diamond-like carbon (ta-C DLC) under boundary lubrication in poly alpha-olefin (PAO) with additives. *Tribol Int* 2013; 65: 286-294. <https://doi.org/10.1016/j.triboint.2013.03.014>.
- [17] Kano M, Yasuda Y, Okamoto Y, Mabuchi Y, Hamada T, Ueno T, Ye J, Konishi S, Takeshima S, Martin JM, De Barros Bouchet MI, Le Mognee T. Ultralow friction of DLC in presence of glycerol mono-oleate (GNO). *Tribol Lett* 2005; 18(2): 245-251. <https://doi.org/10.1007/s11249-004-2749-4>.
- [18] Kaulfuss F, Weihnacht V, Zawischa M, Lorenz L, Makowski S, Hofmann F, Leson A. Effect of Energy and Temperature on Tetrahedral Amorphous Carbon Coatings Deposited by Filtered Laser-Arc. *Materials* 2021; 14(9), 2176. <https://doi.org/10.3390/ma14092176>
- [19] Kuwahara T, Long Y, De Barros Bouchet MI, Martin JM, Moras G, Moseler M. Superlow friction of a-C:H coatings in vacuum: passivation regimes and structural characterization of the sliding interfaces. *Coating* 2021; 11(9): 1069. <https://doi.org/10.3390/coatings11091069>.
- [20] Guibert M, Nauleau B, Kapsa P, Rigaud E. Design and manufacturing of a reciprocating linear tribometre. *Journée Francophones de Tribologie: Tribologie et Couplages Multi-physique*, Lille. Presse Polytechniques et Universitaires Romandes 2006.
- [21] Wagner CD, Davis LE, Zeller MV, Taylor JA, Raymond RH, Gale LH. Empirical atomic sensitivity factors for quantitative analysis by electron spectroscopy for chemical analysis. *Surf Interface Anal* 1981; 3(5): 211-225. <https://doi.org/10.1002/sia.740030506>.
- [22] Long Y, De Barros Bouchet MI, Lubrecht T, Onodera T, Martin JM. Superlubricity of glycerol by self-sustained chemical polishing. *Sci Rep* 2019; 9(1): 1-13. <https://doi.org/10.1038/s41598-019-42730-9>.
- [23] Molchan IS, Thompson GE, Lindsay R, Skeldon P, Likodimos V, Romanos GE, Falaras P, Adamova G, Iliev B, Schubert TJ. Corrosion behaviour of mild steel in 1-alkyl-3-methylimidazolium tricyanomethanide ionic liquids for CO₂ capture applications. *RSC Adv* 2014; 4(11): 5300-5311. <https://doi.org/10.1039/C3RA45872E>.
- [24] Sirivisoot S, Harrison BS. Magnetically stimulated ciprofloxacin release from polymeric microspheres entrapping iron oxide nanoparticles. *Int J Nanomed* 2015; 10: 4447. <https://doi.org/10.2147/ijn.s82830>.
- [25] Yu BZ, Liu XL, Zhang HG, Jing GY, Ma P, Luo Y, Xue WM, Ren ZY, Fan HM. Fabrication and structural optimization of porous single-crystal α -Fe₂O₃ microrices for high-performance lithium-ion battery anodes. *J Mater Chem A* 2015; 3(32): 16544-16550. <https://doi.org/10.1039/C5TA03670D>.
- [26] Williams J. *Engineering tribology*. Cambridge (UK): Cambridge University Press; 2005.
- [27] André E, Vernier C. Some Physical Properties of Pure Ricinoleic Acid: The Refractive Index, Specific Gravity, and Viscosity. *J Rheol* 1932; 3(3): 336-340. <https://doi.org/10.1122/1.2116497>.
- [28] Rabelo J, Batista E, Cavaleri FVW, Meirelles AJ. Viscosity prediction for fatty systems. *J Am Oil Chem Soc* 2000; 77(12): 1255-1262. <https://doi.org/10.1007/s11746-000-0197-z>.
- [29] Kaciulis S. Spectroscopy of carbon: from diamond to nitride films. *Surf Interface Anal* 2012; 44(8): 1155-1161. <https://doi.org/10.1002/sia.4892>.

- [30] Lascovich JC, Scaglione S. Comparison among XAES, PELS and XPS techniques for evaluation of sp^2 percentage in aC: H. *Appl Surf Sci* 1994; 78(1): 17-23. [https://doi.org/10.1016/0169-4332\(94\)90026-4](https://doi.org/10.1016/0169-4332(94)90026-4).
- [31] Lascovich JC, Giorgi R, Scaglione S. Evaluation of the sp^2/sp^3 ratio in amorphous carbon structure by XPS and XAES. *Appl Surf Sci* 1991; 47: 17–21. [https://doi.org/10.1016/0169-4332\(91\)90098-5](https://doi.org/10.1016/0169-4332(91)90098-5).
- [32] Lee SY, Lyu J, Kang S, Lu SJ, Bielawski CW. Ascertaining the carbon hybridization states of synthetic polymers with X-ray induced Auger electron spectroscopy. *J Phys Chem C* 2018; 122(22): 11855-11861. <https://doi.org/10.1021/acs.jpcc.8b02217>.
- [33] Sarangi D, Panwar OS, Kumar S, Bhattacharyya R. Characterization studies of diamond-like carbon films grown using a saddle-field fast-atom-beam source. *J Vac Sci Technol A* 2000; 18(5): 2302-2311. <https://doi.org/10.1116/1.1289699>.
- [34] Noh HJ, Jang H. Friction instability induced by iron and iron oxides on friction material surface. *Wear* 2018; 400: 93-99. <https://doi.org/10.1016/j.wear.2017.12.025>.
- [35] Jayasena DD, Ahn DU, Nam KC, Jo C. Flavour chemistry of chicken meat: A review. *Asian Australas J Anim Sci* 2013; 26(5): 732. <https://doi.org/10.5713/ajas.2012.12619>